

Selective Blocking of Coordination Modes in 1,3,5-Triamino-1,3,5-trideoxy-*cis*-inositol: Enforced Formation of a Low-Spin Iron(III) Hexaamine Complex

Kaspar Hegetschweiler,^{*,1a} Michael Weber,^{1a} Volker Huch,^{1a} Michael Veith,^{1a} Helmut W. Schmalke,^{1b} Anthony Linden,^{1c} Rodney J. Geue,^{1d,e} Peter Osvath,^{1d,f} Alan M. Sargeson,^{1d,e} Anthony C. Willis,^{1d} and Werner Angst^{1g}

Universität des Saarlandes, Anorganische Chemie, D-66041 Saarbrücken, Germany, Anorganisch-Chemisches Institut, Universität Zürich, Winterthurerstrasse 190, CH-8057 Zürich, Switzerland, Organisch-Chemisches Institut, Universität Zürich, Winterthurerstrasse 190, CH-8057 Zürich, Switzerland, Research School of Chemistry, Australian National University, Canberra, ACT 0200, Australia, and EAWAG, CH-8600 Dübendorf, Switzerland

Received March 13, 1997[⊗]

[Fe(tmca)₂]³⁺ and [Co(tmca)₂]³⁺ (tmca = all-*cis*-2,4,6-trimethoxycyclohexane-1,3,5-triamine) were prepared and characterized by elemental analyses, NMR, and FAB⁺ mass spectrometry and by spectroscopic methods (UV–vis). Magnetic susceptibility measurements established a low-spin d⁵ electron configuration for the Fe^{III} hexaamine complex. In aqueous solution, cyclic voltammetry revealed a quasi reversible one electron reduction for both complexes with M^{III}/M^{II} redox potentials of +0.16 and –0.30 V (vs SHE), respectively. The two compounds [M(tmca)₂]Cl₃·5H₂O·EtOH (C₂₀H₅₈Cl₃MN₆O₁₂, M = Fe, Co) are isostructural. They both crystallize in the triclinic space group *P* $\bar{1}$, *Z* = 2. Fe complex: *a* = 10.338(3) Å, *b* = 13.062(4) Å, *c* = 14.042(4) Å, α = 80.20(2)°, β = 72.07(2)°, γ = 69.11(2)°. Co complex: *a* = 10.307(3) Å, *b* = 13.066(2) Å, *c* = 14.029(2) Å, α = 80.14(1)°, β = 72.18(2)°, γ = 69.55(2)°. The ligand tmca is compared with the unsubstituted 1,3,5-triamino-1,3,5-trideoxy-*cis*-inositol (taci) and the N-methylated 1,3,5-trideoxy-1,3,5-tris(dimethylamino)-*cis*-inositol (tdci). Due to the methyl groups on the oxygen donors, tmca binds both Fe^{III} and Co^{III} ions exclusively via nitrogen donors whereas the previously reported [Fe(tdci)₂]³⁺ had an FeO₆ coordination environment. Equilibration of a 1:1 mixture of [Fe(tdci)₂]³⁺ and [Fe(tmca)₂]³⁺ in aqueous solution resulted in the quantitative formation of the metathesis product [Fe(tmca)(tdci)]Cl₃·15H₂O (O₃N₃ coordination). Crystal data: C₂₁H₇₈Cl₃FeN₆O₂₁, trigonal, space group *R*3*c*, *a* = 15.158(2) Å, *c* = 33.591(7) Å, *Z* = 6. The differences in the structural properties of the low-spin hexaamine [Fe(tmca)₂]³⁺ complex and the high-spin [Fe(tdci)₂]³⁺ and [Fe(tmca)(tdci)]³⁺ complexes are discussed.

Introduction

In a recent publication,² we reported the preparation and characterization of [Fe(taci)₂]³⁺ (**1**, taci = 1,3,5-triamino-1,3,5-trideoxy-*cis*-inositol) in the solid state and in aqueous solution. A “double-adamantane” type structure was observed, where one ligand binds the ferric ion via three axial amino groups, while the other ligand coordinates via three axial alkoxy groups. Complex **1** is an illustrative example which demonstrates the unique versatility of taci in providing either nitrogen or oxygen donors for metal ion binding (Scheme 1). Individual coordination properties of metal centers are clearly reflected in their interactions with taci: In the bis-complexes of the alkali metal and alkaline earth metal cations, both ligands coordinate the metal ions exclusively via oxygen donors.^{3,4} This is also true for Al^{III}, Ti^{IV}, Ge^{IV}, and Sn^{IV}, although as a consequence of the higher charge of these metal ions, taci coordinates as a zwitterion

with deprotonated hydroxy groups and protonated nitrogen atoms.^{5,6} On the other hand, the divalent transition metals from Mn^{II} to Cu^{II}, as well as Zn^{II}, Cd^{II} and Tl^{III}, all form bis-complexes with MN₆ coordination,^{3,5–7} whereas the mixed MN₃O₃ structure observed for Fe^{III} has also been found for Cr^{III} and Ga^{III}.^{5,8}

The selectivity of the ligand can be readily tuned by introducing more bulky substituents on either the oxygen or nitrogen donors of taci. In 1,3,5-trideoxy-1,3,5-tris(dimethylamino)-*cis*-inositol (tdci), the conformer with three axial dimethylamino groups is destabilized by nonbonding (*intraligand*) repulsions and only the conformation with three axial hydroxy groups is available for metal binding.^{9,10} Also additional *interligand* repulsion between the dimethylamino groups would substantially increase steric strain in a bis-complex of tdci with MN₆ coordination.³ Consequently, exclusive FeO₆ coordination is observed for [Fe(tdci)₂]³⁺ (**2**). Similar considerations should be valid for the all-*cis*-2,4,6-trimethoxycyclohexane-1,3,5-triamine (tmca), where exclusive coordination by three axial nitrogen atoms is to be expected. Now, we report single-crystal

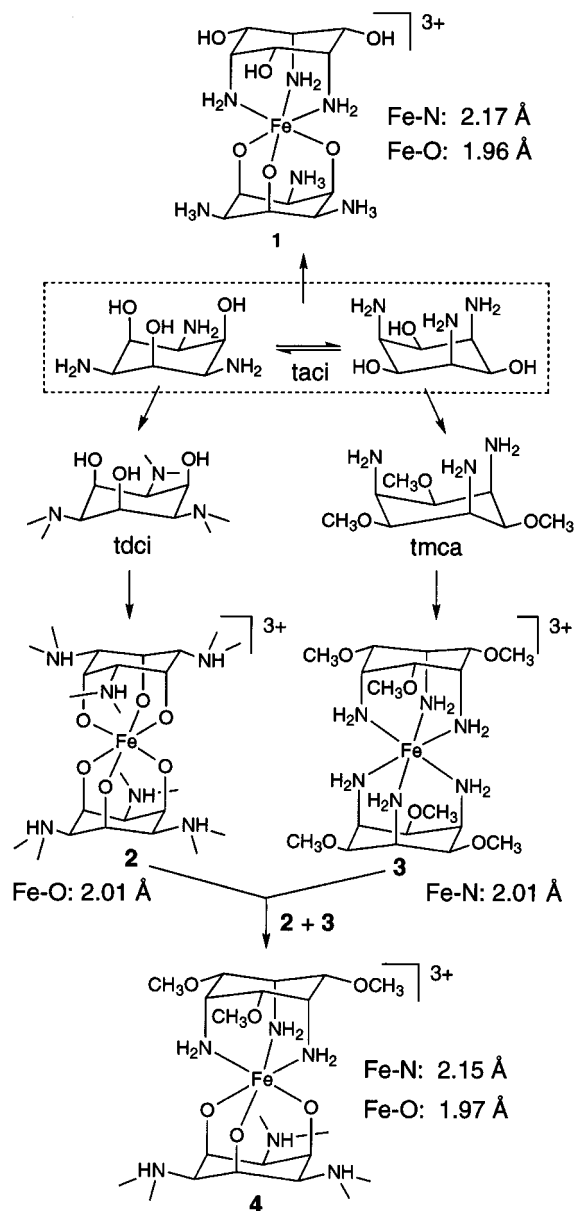
* To whom correspondence should be addressed.

⊗ Abstract published in *Advance ACS Abstracts*, August 1, 1997.

- (1) (a) Universität des Saarlandes. (b) Anorganisch-Chemisches Institut, Universität Zürich. (c) Organisch-Chemisches Institut, Universität Zürich. (d) Australian National University. (e) Present address: Department of Chemistry, Faculty of Science, Australian National University, Canberra, ACT 0200, Australia. (f) Present address: CSIRO Ian Wark Laboratory, Clayton, VIC 3169, Australia. (g) EAWAG.
 (2) Hegetschweiler, K.; Ghisletta, M.; Hausherr-Primo L.; Kradolfer, T.; Schmalke, H. W.; Gramlich, V. *Inorg. Chem.* **1995**, *34*, 1950.
 (3) Hegetschweiler, K.; Hancock, R. D.; Ghisletta, M.; Kradolfer, T.; Gramlich, V.; Schmalke, H. W. *Inorg. Chem.* **1993**, *32*, 5273.
 (4) Kradolfer, T. Thesis, Diss. No. 10935, ETH-Zürich, Switzerland, 1995.

- (5) Hegetschweiler, K.; Ghisletta, M.; Fässler, T. F.; Nesper, R.; Schmalke, H. W.; Rihs, G. *Inorg. Chem.* **1993**, *32*, 2032.
 (6) Ghisletta, M. Thesis, Diss. No. 10891, ETH-Zürich, Switzerland, 1994.
 (7) Hegetschweiler, K.; Gramlich, V.; Ghisletta, M.; Samaras, H. *Inorg. Chem.* **1992**, *31*, 2341.
 (8) Schmalke, H. W.; Hegetschweiler, K.; Ghisletta, M. *Acta Crystallogr.* **1991**, *C47*, 2047.
 (9) Hegetschweiler, K.; Kradolfer, T.; Gramlich, V.; Hancock, R. D. *Chem. Eur. J.* **1995**, *1*, 74.
 (10) Kradolfer, T.; Hegetschweiler, K. *Helv. Chim. Acta* **1992**, *75*, 2243.

Scheme 1



X-ray analyses for trichloride salts of $[\text{Fe}(\text{tmca})_2]^{3+}$ (**3**), the mixed $[\text{Fe}(\text{tmca})(\text{tdci})]^{3+}$ (**4**), and $[\text{Co}(\text{tmca})_2]^{3+}$ (**5**) and compare their structural properties with the Fe^{III} *taci* and *tdci* complexes **1** and **2** and with $[\text{Co}(\text{taci})_2]^{3+}$ (**6**).¹¹

Experimental Section

Physical Measurements. Cyclic voltammograms were carried out with the usual three-electrode configuration with a calomel reference electrode (saturated KCl), a Pt counter electrode, a Au working electrode, and a BAS 100 electrochemistry system. All measurements were performed in 0.1 M NaCl (aqueous) at $23 \pm 1^\circ\text{C}$. The potentials are quoted versus the standard hydrogen electrode SHE. UV-vis spectra were recorded with a Uvikon 820 spectrophotometer. ^1H and ^{13}C NMR spectra were measured in D_2O at 28°C on a Varian Gemini 300 MHz Fourier transform NMR spectrometer. Chemical shifts (in ppm) are given relative to sodium (trimethylsilyl)propionate- d_4 (=0 ppm) as internal standard. FAB⁺ mass spectra were recorded on a VG ZAB VSEQ instrument. Test solutions were prepared by dissolving the samples in water and mixing the resulting solutions with a glycerol matrix prior to introduction into the spectrometer. Magnetic suscep-

tibility measurements were performed on an MPMS 5 SQUID magnetometer (Quantum Design) at a magnetic field of 1000 G. Diamagnetic corrections were applied with the use of published tables.

Materials and Analyses. $\text{CoCl}_2 \cdot 6\text{H}_2\text{O}$, FeCl_3 (anhydrous), and the organic solvents were commercially available products of reagent grade quality. They were used without further purification. $[\text{Fe}(\text{tdci})_2]\text{Cl}_3 \cdot 15\text{H}_2\text{O}$ was prepared according to a previously described procedure.¹⁰ $\text{tmca} \cdot 3\text{HCl}$ was prepared by selective O-methylation of 1,3,5-triamino-1,3,5-trideoxy-*cis*-inositol.¹² Anal. Calc for $\text{C}_9\text{H}_{24}\text{Cl}_3\text{N}_3\text{O}_3$: C, 32.89; H, 7.36; N, 12.78. Found: C, 32.73; H, 7.35; N, 12.62. ^1H NMR (pH 2): 3.55 (s, 9H), 3.77 (t, 3H, $J = 3.6$ Hz), 4.05 (t, 3H, $J = 3.6$ Hz). ^{13}C NMR (pH 2): 53.5, 65.5, 77.6. Dowex 50 W-X2 (100–200 mesh, H^+ form) was from Fluka. Dowex 2-X8 (50–100 mesh, OH^- form) was obtained from the corresponding Cl^- form (from Fluka) by elution with 0.2 M NaOH. C, H, and N analyses were performed by D. Manser, Laboratorium für Organische Chemie, ETH Zürich. Fe analyses (atomic absorption) were measured by K. Hametner, Laboratorium für Anorganische Chemie, ETH Zürich.

Solid Salts of $[\text{Fe}(\text{tmca})_2]^{3+}$. $\text{tmca} \cdot 3\text{HCl}$ (490 mg, 1.49 mmol) was dissolved in 25 mL of water and deprotonated using Dowex 2 (40 cm^3 , OH^- form). The solution was evaporated to dryness under reduced pressure, and the oily residue was dried in vacuo at room temperature for 2 days. The resulting white solid was dissolved in 50 mL of dry MeOH. A solution of FeCl_3 (118 mg, 0.73 mmol) in 20 mL of dry MeOH was then added. The clear orange solution was evaporated under reduced pressure to a total volume of 5 mL. A solid product was precipitated by the addition of 70 mL of dry acetone and recrystallized from boiling 2-propanol. The resulting crystals of the composition $[\text{Fe}(\text{tmca})_2]\text{Cl}_3 \cdot 6\text{C}_3\text{H}_7\text{OH} \cdot \text{H}_2\text{O}$ were, however, not stable in air.¹³ They were dried in vacuo at ambient temperature for 3 days, yielding 0.30 g (66%) of $[\text{Fe}(\text{tmca})_2]\text{Cl}_3 \cdot \text{H}_2\text{O}$. Anal. Calc for $\text{C}_{18}\text{H}_{44}\text{Cl}_3\text{FeN}_6\text{O}_7$: C, 34.94; H, 7.17; N, 13.58; Fe, 9.03. Found: C, 34.94, H, 7.14, N, 13.78, Fe 9.02. MS (FAB⁺): m/e 655.1 (7%, $[\text{Fe}_2\text{L}_2\text{Cl}_3]^+$), 529.3 (28%, $[\text{FeL}_2\text{Cl}]^+$), 493.3 (23%, $[\text{FeL}_2 - \text{H}]^+$), 310.1 (100%, $[\text{FeLCl}]^+$),¹⁴ 274.1 (32%, $[\text{FeL} - \text{H}]^+$), 220.1 (22%, $[\text{HL}]^+$). ^1H NMR: 4.56 (s).¹⁵ Magnetic and vis-spectroscopic data are given in the results section. Stable crystals of the composition $[\text{Fe}(\text{tmca})_2]\text{Cl}_3 \cdot 5\text{H}_2\text{O} \cdot \text{EtOH}$, suitable for single-crystal X-ray analysis, were grown from wet EtOH at 4°C . The complex was also crystallized as the tetrachlorozincate: 100 mg (0.16 mmol) of $[\text{Fe}(\text{tmca})_2]\text{Cl}_3 \cdot \text{H}_2\text{O}$ was dissolved in 10 mL of water. A solution of ZnCl_2 (220 mg, 1.61 mmol) in 10 mL of 2 M aqueous HCl was added, resulting in the deposition of orange crystals.¹⁶ Yield: 104 mg (71%) of $[\text{Fe}(\text{tmca})_2]_2\text{[ZnCl}_4]_3 \cdot 12\text{H}_2\text{O}$. Calc for $\text{C}_{36}\text{H}_{108}\text{Cl}_{12}\text{Fe}_2\text{N}_{12}\text{O}_{24}\text{Zn}_3$: C, 23.67; H, 5.96; N, 9.20. Found: C, 23.62, H, 5.66, N, 9.12.

$[\text{Fe}(\text{tmca})(\text{tdci})]\text{Cl}_3 \cdot 15\text{H}_2\text{O}$. A mixture of $[\text{Fe}(\text{tmca})_2]\text{Cl}_3 \cdot \text{H}_2\text{O}$ (103 mg, 0.17 mmol) and $[\text{Fe}(\text{tdci})_2]\text{Cl}_3 \cdot 15\text{H}_2\text{O}$ (160 mg, 0.17 mmol) was

- (12) Weber, M. Thesis, Diss. No. 12071, ETH-Zürich, Switzerland, 1997.
- (13) $[\text{Fe}(\text{tmca})_2]_2\text{Cl}_6 \cdot 12\text{C}_3\text{H}_7\text{OH} \cdot 2\text{H}_2\text{O}$ crystallizes in a triclinic crystal system with cell dimensions $a = 14.358(3)\text{ \AA}$, $b = 14.875(3)\text{ \AA}$, $c = 15.059(4)\text{ \AA}$, $\alpha = 61.45(2)^\circ$, $\beta = 69.40(2)^\circ$, $\gamma = 87.07(2)^\circ$, $Z = 1$ (for $\text{C}_{72}\text{H}_{184}\text{Cl}_6\text{Fe}_2\text{N}_{12}\text{O}_{26}$). Although two $[\text{Fe}(\text{tmca})_2]^{3+}$ entities could be located unambiguously, the result of the refinement in the space groups $P1$ and $P1$ was not satisfactory ($P1$: $R = 8.16\%$ for 6915 observed reflections with $I \geq 2\sigma(I)$ and $wR_2 = 28.4\%$ for all 11 979 data and 663 refined parameters).
- (14) The agreement between the calculated isotope distribution (I_{calcd}) of $[\text{FeLCl}]^+$ and the measured intensities I_{obs} in the range $308 \leq m/z \leq 313$ was $R = \sum |I_{\text{calcd}} - I_{\text{obs}}| / \sum I_{\text{obs}} = 0.26$. This value decreased to $R = 0.12$ by considering $[\text{FeLCl} - \text{H}]^+$ (14%) and $[\text{FeLCl} + \text{H}]^+$ (9%) as additional species (least-squares refinement). This implies, however, the simultaneous presence of Fe^{III} , Fe^{II} , and Fe^{I} (see refs 9 and 10).
- (15) The ^1H NMR spectrum of **3** showed only one slightly broadened singlet with a line width of about 5 Hz which was assigned to the six methoxy groups. The protons of the two cyclohexane rings, which are much closer to the paramagnetic center, could not be observed in the range 0–14 ppm. In 1 M DCl, liberation of free $\text{H}_3\text{tmca}^{3+}$ was indicated by increasing signals at 4.05 ppm (t, 3H), 3.77 (t, 3H), and 3.55 (s, 9H).
- (16) $[\text{Fe}(\text{tmca})_2]_2[\text{ZnCl}_4]_3 \cdot 12\text{H}_2\text{O}$ crystallizes in the triclinic space group $P1$, with $a = 9.999(2)\text{ \AA}$, $b = 10.891(2)\text{ \AA}$, $c = 18.310(4)\text{ \AA}$, $\alpha = 85.02(3)^\circ$, $\beta = 88.25(3)^\circ$, $\gamma = 74.01(3)^\circ$, $\text{C}_{18}\text{H}_{54}\text{Cl}_6\text{FeN}_6\text{O}_{12}\text{Zn}_{1.5}$, $Z = 2$, and $R = 6.81\%$ for 4621 observed reflections with $I > 2\sigma(I)$ and $wR_2 = 25.5\%$ (for all 5008 data) and 441 refined parameters (Siemens Stoe AED 2 four-circle diffractometer, graphite-monochromated Mo K α radiation).

(11) Ghisletta, M.; Jalett, H.-P.; Gerfin, T.; Gramlich, V.; Hegetschweiler, K. *Helv. Chim. Acta* **1992**, *75*, 2233.

Table 1. Crystallographic Data for [Fe(tmca)₂]Cl₃·5H₂O·EtOH (**3**), [Fe(tmca)(tdci)]Cl₃·15H₂O (**4**), and [Co(tmca)₂]Cl₃·5H₂O·EtOH (**5**)

| | complex | | |
|--|--|--|--|
| | 3 | 4 | 5 |
| chem formula | C ₂₀ H ₅₈ Cl ₃ FeN ₆ O ₁₂ | C ₂₁ H ₇₈ Cl ₃ FeN ₆ O ₂₁ | C ₂₀ H ₅₈ Cl ₃ CoN ₆ O ₁₂ |
| fw | 736.9 | 913.1 | 740.0 |
| space group | <i>P</i> $\bar{1}$ (No. 2) | <i>R</i> 3 <i>c</i> (No. 161) | <i>P</i> $\bar{1}$ (No. 2) |
| <i>a</i> , Å | 10.338(3) | 15.158(2) | 10.307(3) |
| <i>b</i> , Å | 13.062(4) | 15.158(2) | 13.066(2) |
| <i>c</i> , Å | 14.042(4) | 33.591(7) | 14.029(2) |
| α , deg | 80.20(2) | 90 | 80.14(1) |
| β , deg | 72.07(2) | 90 | 72.18(2) |
| γ , deg | 69.11(2) | 120 | 69.55(2) |
| <i>V</i> , Å ³ | 1681.6(9) | 6684(2) | 1680.9(7) |
| <i>Z</i> | 2 | 6 | 2 |
| <i>T</i> , °C | 20 | 20 | 23 |
| λ , Å | 0.710 73 | 0.710 73 | 0.710 73 |
| ρ_{calc} , g cm ⁻³ | 1.46 | 1.36 | 1.46 |
| μ , cm ⁻¹ | 7.49 | 5.94 | 8.11 |
| <i>R</i> ^a | 0.0434 ^b | 0.0386 ^b | 0.036 ^c |
| <i>R</i> _w [<i>I</i> > 3 σ (<i>I</i>)] ^d | | | 0.031 |
| <i>wR</i> ₂ (all data) ^e | 0.1305 | 0.1027 | |

^a $R = \sum ||F_o| - |F_c|| / \sum |F_o|$. ^b $I > 2\sigma(I)$. ^c $I > 3\sigma(I)$. ^d $R_w = [\sum w(|F_o| - |F_c|)^2 / \sum w F_o^2]^{1/2}$. ^e $wR_2 = [\sum w(F_o^2 - F_c^2)^2 / \sum w F_o^4]^{1/2}$.

dissolved in 30 mL of water and stirred for 12 h at 90 °C. A color change from orange to pale yellow was noted. The solution was evaporated to dryness under reduced pressure. The resulting solid was redissolved in a small volume of 2-propanol and filtered hot. After cooling to 0 °C, yellow crystals were formed. These had the composition [Fe(tmca)(tdci)]Cl₃·15H₂O, and they were suitable for single-crystal X-ray analysis. Drying in vacuo yielded the monohydrate [Fe(tmca)(tdci)]Cl₃·H₂O (82%). Calc for C₂₁H₅₀Cl₃FeN₆O₇: C, 38.17; H, 7.63; N, 12.72. Found: C, 37.97, H, 7.35, N, 12.74. MS (FAB⁺): *m/e* 534.3 (100%, [Fe(tmca)(tdci) - 2H]⁺). Equilibration of the dried product in humid air (60% atmospheric moisture, 23 °C) resulted in the formation of [Fe(tmca)(tdci)]Cl₃·14.5H₂O, indicating an almost complete, reversible uptake of the lost water of crystallization. Calc for C₂₁H₇₇Cl₃FeN₆O_{20.5}: C, 27.90; H, 8.58; N, 9.30. Found: C, 27.89, H, 8.57, N, 9.52.

[Co(tmca)₂]Cl₃·5H₂O·EtOH. Solid tmca·3HCl (4.5 g, 13.7 mmol) was dissolved in 100 mL of water. Solid NaOH (1.50 g) and CoCl₂·6H₂O (1.35 g), dissolved in 30 mL of water, were then added, and a pale orange solution of [Co(tmca)₂]Cl₂ was obtained. The solution was stirred at 60 °C, and air was passed through the reaction mixture for 4 h. The resulting dark orange solution was diluted with water to a total volume of 1.5 L and sorbed onto Dowex 50 W-X2. The column was washed with water and then 0.5 M HCl. Elution with 3 M HCl yielded an orange fraction which was evaporated to dryness, and the residue was suspended in 150 mL of EtOH. The suspension was filtered, yielding a small amount of the blue solid [Co(tmca)Cl₃] and a clear orange solution. The orange solution was evaporated to dryness under reduced pressure, yielding pure, solid [Co(tmca)₂]Cl₃·H₂O (77%). Anal. Calc for C₁₈H₄₄Cl₃CoN₆O₇: C, 34.77; H, 7.13; N, 13.51. Found: C, 34.63; H, 7.01; N, 13.40. UV-vis (λ_{max}): 342 nm ($\epsilon = 76 \text{ M}^{-1} \text{ cm}^{-1}$), 472 nm ($\epsilon = 77 \text{ M}^{-1} \text{ cm}^{-1}$). ¹H NMR: 5.00 (br, 12 H), 3.62 (m, 6H), 3.47 (s, 18 H), 3.24 (t, 6H t, *J* = 3.6 Hz). ¹³C NMR: 74.9, 60.1, 46.8. MS (FAB⁺): *m/e* 313.1 (100%, [Co(tmca)Cl]⁺), 495.3 (66%, [Co(tmca)₂ - 2H]⁺), 661.1 (11%, [Co₂(tmca)₂Cl₃]⁺). Single crystals of the composition [Co(tmca)₂]Cl₃·5H₂O·EtOH were grown from a saturated EtOH solution at 4 °C.

Crystal Structure Determination. Crystal data are presented in Table 1. Atomic coordinates are available as Supporting Information. Selected bond distances and bond angles are listed in Tables 2–4. Additional information on data collection, structure solution, and refinement is summarized below.

Data for [Co(tmca)₂]Cl₃·5H₂O·EtOH (chloride salt of **5**) were collected at 23 ± 1 °C on an orange crystal, having approximate dimensions of 0.36 × 0.24 × 0.11 mm using a Rigaku AFC6S diffractometer and graphite monochromated Mo K α radiation. Three standard reflections were measured after every 150 reflections. Over the course of data collection, the standards decreased by 2.4%. A linear correction factor was applied to the data to account for this phenomenon. An analytical absorption correction was applied, and the data were

Table 2. Selected Bond Lengths (Å) and Angles (deg) of [Fe(tmca)₂]³⁺ (**3**) with Esd's in Parentheses

| | | | |
|----------------|------------|----------------|------------|
| Fe–N(11) | 2.019(2) | N(11)–C(11) | 1.487(3) |
| Fe–N(31) | 2.010(2) | N(31)–C(31) | 1.479(3) |
| Fe–N(51) | 2.023(2) | N(51)–C(51) | 1.489(3) |
| Fe–N(12) | 2.007(2) | N(12)–C(12) | 1.483(3) |
| Fe–N(32) | 2.007(2) | N(32)–C(32) | 1.484(3) |
| Fe–N(52) | 2.020(2) | N(52)–C(52) | 1.486(3) |
| N(12)–Fe–N(32) | 90.45(8) | N(12)–Fe–N(31) | 89.74(8) |
| N(32)–Fe–N(31) | 179.15(8) | N(12)–Fe–N(11) | 178.17(8) |
| N(32)–Fe–N(11) | 91.36(8) | N(31)–Fe–N(11) | 88.45(8) |
| N(12)–Fe–N(52) | 89.07(8) | N(32)–Fe–N(52) | 88.25(8) |
| N(31)–Fe–N(52) | 90.92(8) | N(11)–Fe–N(52) | 91.25(8) |
| N(12)–Fe–N(51) | 90.46(8) | N(32)–Fe–N(51) | 90.49(8) |
| N(31)–Fe–N(51) | 90.34(8) | N(11)–Fe–N(51) | 89.25(8) |
| N(52)–Fe–N(51) | 178.65(7) | C(11)–N(11)–Fe | 119.36(13) |
| C(31)–N(31)–Fe | 118.94(13) | C(51)–N(51)–Fe | 118.41(13) |
| C(12)–N(12)–Fe | 118.93(13) | C(32)–N(32)–Fe | 119.28(13) |
| C(52)–N(52)–Fe | 119.08(13) | | |

Table 3. Selected Bond Lengths (Å) and Angles (deg) of [Fe(tmca)(tdci)]³⁺ (**4**) with Esd's in Parentheses

| | | | |
|-----------------------------|----------|-----------------------------|----------|
| Fe–O(22) | 1.967(3) | Fe–N(11) | 2.152(4) |
| O(21)–C(21) | 1.425(5) | O(21)–C(71) | 1.436(5) |
| O(22)–C(22) | 1.398(5) | N(11)–C(11) | 1.487(5) |
| N(12)–C(12) | 1.525(5) | | |
| O(22)–Fe–O(22) ^a | 91.5(1) | O(22)–Fe–N(11) ^b | 82.8(1) |
| O(22)–Fe–N(11) ^a | 103.0(1) | N(11)–Fe–O(22) | 164.5(1) |
| N(11)–Fe–N(11) ^a | 84.5(2) | Fe–O(22)–C(22) | 117.9(2) |
| Fe–N(11)–C(11) | 121.3(3) | | |

^a Symmetry operation to generate equivalent atoms: (a) $-x + y, -x, z$; (b) $-y, x - y, z$.

corrected for Lorentz and polarization effects. The structure was solved by Patterson methods and expanded using Fourier techniques. Hydrogen atoms attached to carbon atoms were placed at calculated positions. The remaining hydrogen atoms were located in difference Fourier maps and their coordinates refined with fixed displacement parameters by full-matrix least-squares calculations using the teXsan¹⁷ program. The displacement ellipsoids of C(82) and C(2e) appeared to be unusually large, indicating some disorder; however, the refinement of the structure with two partially occupied sites for each atom did not give a better agreement and was therefore discarded.

Orange crystals of [Fe(tmca)₂]Cl₃·5H₂O·EtOH (chloride salt of **3**) were all visibly twinned. A single untwinned platelet of approximate size 0.62 × 0.32 × 0.12 mm was carefully cut from one of these crystals.

(17) teXsan, Crystal Structure Analysis Package, Molecular Structure Corp., 1992.

Table 4. Selected Bond Lengths (Å) and Angles (deg) of [Co(tmca)₂]³⁺ (**5**) with Esd's in Parentheses

| | | | |
|----------------|----------|----------------|----------|
| Co–N(11) | 1.992(3) | N(11)–C(11) | 1.486(4) |
| Co–N(31) | 1.983(3) | N(31)–C(31) | 1.484(4) |
| Co–N(51) | 1.988(3) | N(51)–C(51) | 1.489(4) |
| Co–N(12) | 1.978(3) | N(12)–C(12) | 1.483(4) |
| Co–N(32) | 1.978(3) | N(32)–C(32) | 1.490(4) |
| Co–N(52) | 1.982(3) | N(52)–C(52) | 1.492(4) |
| N(11)–Co–N(31) | 89.1(1) | N(11)–Co–N(51) | 89.7(1) |
| N(11)–Co–N(12) | 178.5(1) | N(11)–Co–N(32) | 90.9(1) |
| N(11)–Co–N(52) | 90.7(1) | N(31)–Co–N(51) | 90.6(1) |
| N(31)–Co–N(12) | 89.4(1) | N(31)–Co–N(32) | 179.4(1) |
| N(31)–Co–N(52) | 90.7(1) | N(51)–Co–N(12) | 90.2(1) |
| N(51)–Co–N(32) | 90.0(1) | N(51)–Co–N(52) | 178.6(1) |
| N(12)–Co–N(32) | 90.6(1) | N(12)–Co–N(52) | 89.5(1) |
| N(32)–Co–N(52) | 88.7(1) | Co–N(11)–C(11) | 119.3(2) |
| Co–N(31)–C(31) | 119.0(2) | Co–N(51)–C(51) | 118.7(2) |
| Co–N(12)–C(12) | 119.1(2) | Co–N(32)–C(32) | 119.5(2) |
| Co–N(52)–C(52) | 119.7(2) | | |

The unit cell parameters were almost identical with those of the cobalt analogue (**5**). Data collection was performed at 20 ± 1 °C on an Enraf-Nonius CAD-4 diffractometer using graphite-monochromated Mo K α radiation. A total of 10 263 (including 111 standards) intensity data were collected ($3.0^\circ < 2\theta < 60.0^\circ$), using the ω - 2θ scan mode with variable scan speeds. A linear decay of up to 4.5% was observed during data collection. Data reduction (9782 unique reflections, $R_{\text{int}} = 0.0175$), LP corrections, a numerical absorption correction based on six indexed crystal faces, and a decay correction were applied. The atomic coordinates of the Co analogue were used for an initial isotropic least-squares refinement. Two distinct positions were located for C(82) in a difference Fourier map, and they were refined as split positions C(82A) and C(82B) with isotropic displacement parameters, having occupancies of 0.62(2) and 0.38(2), respectively. Additional disorder was observed for C(2e); however, the representation of the structure by partially occupied sites did not result in a chemically meaningful model and the atom was therefore described by one single position and refined in the anisotropic mode. The positions of all H atoms were located in a difference electron density map. The positions of the methyl hydrogen atoms of the tmca ligands and of the EtOH group were refined using a riding model with fixed C–H distances of 0.96 Å (SHELXL-93).¹⁸ All other H atoms were refined freely with isotropic displacement parameters. In the final refinement 9782 reflections were used and 536 parameters refined; $\text{gof} = 1.115$, $\Delta/\sigma_{\text{(max)}} = 0.008$, and residual electron density = 0.83 and $-0.71 \text{ e}\text{\AA}^{-3}$.

Data for [Fe(tmca)(tdci)]Cl₃·15H₂O (chloride salt of **4**) were collected at 20 ± 2 °C on a pale yellow prism having approximate dimensions of $0.2 \times 0.2 \times 0.08$ mm using a Siemens Stoe AED 2 four-circle diffractometer and graphite-monochromated Mo K α radiation. No crystal decay was observed during data collection. A semi-empirical absorption correction (ψ -scans) was applied. The minimum and maximum transmission factors were 0.8454 and 0.9953. The structure was solved by direct methods (SHELXS-86)¹⁹ and refined by full-matrix least-squares calculations (SHELXL-93, 1954 independent reflections, 209 parameters)¹⁸ using anisotropic displacement parameters for all non-hydrogen positions. The hydrogen atomic positions of the complex were calculated (riding model). The hydrogen atoms of the H₂O molecules could be located in a difference Fourier map and were refined with isotropic displacement parameters.

Results and Discussion

Preparation, Characterization, and Reactivity in Aqueous Solution. [Co(tmca)₂]³⁺ (**5**) was obtained in good yield by the usual procedure (air oxidation of Co²⁺ in the presence of a slight excess of the partially protonated ligand dissolved in water).¹¹ It was possible to prepare the corresponding [Fe(tmca)₂]³⁺ complex (**3**) in poor yield by the same procedure, but direct synthesis, starting from anhydrous FeCl₃ and tmca in dry MeOH,

was more efficient. Both complexes were isolated as solid salts and were characterized by elemental analysis, FAB⁺ mass spectrometry,¹⁴ and vis and NMR spectroscopy.¹⁵ The vis spectrum of the Fe^{III} complex **3** in H₂O showed maxima at 349 nm ($\epsilon = 211 \text{ M}^{-1} \text{ cm}^{-1}$), 408 nm (shoulder, $\epsilon = 56 \text{ M}^{-1} \text{ cm}^{-1}$), 441 nm ($\epsilon = 50 \text{ M}^{-1} \text{ cm}^{-1}$), and 522 nm (shoulder, $\epsilon = 21 \text{ M}^{-1} \text{ cm}^{-1}$). The effective magnetic moment (μ_{eff}) increased monotonically from 1.98 μ_{B} (3 K) to 2.78 μ_{B} (300 K) displaying a significant orbital contribution at 300 K. All these spectroscopic and magnetic properties are in close agreement with those reported for other low-spin Fe^{III} hexamine complexes.²⁰

As expected, the Co complex **5** is quite inert and ligand dissociation could not be detected in aqueous solution at all. By contrast, the Fe^{III} complex **3** is somewhat more labile. In 1 M DCl, slow formation of the free ligand with a half-life of about 4–6 weeks was observed over a period of a few months at 23 ± 2 °C using NMR spectroscopy.¹⁵ Addition of base to a neutral or slightly acidic aqueous solution of **3** resulted in an immediate color change from yellow to dark purple. By analogy with the reaction of [Fe(tacn)₂]³⁺ (tacn = 1,4,7-triazacyclononane), reported by Pohl et al.,²¹ we formulate this reaction as the deprotonation of a coordinated amino group. As expected for a simple deprotonation, this reaction is completely reversible. However, at very high base concentration (pH > 13), the deep purple color faded rapidly and a colorless solution resulted, followed by the formation of a brown solid (FeOOH) as the final product. We tentatively formulate the colorless intermediate as a neutral high-spin complex [Fe(tmca)(OH)₃] with a mixed O₃N₃ donor set²¹ according to [Fe(tmca)₂]³⁺ (yellow) → [Fe(tmca)(H₋₁tmca)]²⁺ (deep purple) → [Fe(tmca)(OH)₃] (colorless) → FeOOH(s) (brown). The dramatically increased rate of ligand dissociation in alkaline solution is in accord with the well-known base catalysis (S_N1CB mechanism), observed for many amine complexes.²² The preference for a mixed O₃N₃-coordination environment for high-spin Fe^{III} has already been noted for [Fe(taci)₂]³⁺² and was confirmed here by the facile formation of [Fe(tmca)(tdci)]³⁺, which was obtained almost quantitatively by a simple metathesis reaction of **2** and **3** (Scheme 1).

The redox properties of the two complexes **3** and **5** were investigated by cyclic voltammetry in aqueous solution. The cyclic voltammograms of both complexes showed quasi reversible one-electron M^{III} ⇌ M^{II} reduction and oxidation. The redox potentials are +0.16(1) V ($\Delta E_{\text{p}} = 66 \text{ mV}$) for the Fe complex **3**, and $-0.30(1) \text{ V}$ ($\Delta E_{\text{p}} = 88 \text{ mV}$) for the Co complex **5** (vs SHE, 0.1 M aqueous NaCl, gold working electrode). These values are very similar to those of comparable low-spin Fe^{III} and Co^{III} hexamine complexes.²³

Crystal Structures. Single crystals of the composition [Fe(tmca)₂]₂Cl₆·2H₂O·12i-PrOH were obtained from 2-propanol, but they proved to be unstable in air and disintegrated rapidly. Moreover, an X-ray analysis, performed at -100 °C, revealed a severely disordered structure.¹³ The complex was therefore crystallized as a tetrachlorozincate salt of the composition [Fe(tmca)₂]₂[ZnCl₄]₃·12H₂O from aqueous solution, but X-ray analysis revealed disorder in one of the ZnCl₄²⁻ counterions which could not be described satisfactorily.¹⁶ Further crystal-

(18) Sheldrick, G. M. SHELXL-93, a program for the refinement of X-ray structures, University of Göttingen, 1993.

(19) Sheldrick, G. M. SHELXS-86. *Acta Crystallogr.* **1990**, *A46*, 467.

(20) Renovitch, G. A.; Baker, W. A., Jr. *J. Am. Chem. Soc.* **1968**, *90*, 3585. Wiegardt, K.; Tolksdorf, I.; Herrmann, W. *Inorg. Chem.* **1985**, *24*, 1230. See also refs 23 and 25d.

(21) Pohl, K.; Wiegardt, K.; Kaim, W.; Steenzen, S. *Inorg. Chem.* **1988**, *27*, 440.

(22) Tobe, M. L. *Adv. Inorg. Bioinorg. Mech.* **1983**, *2*, 1 and references therein.

(23) A value of 0.13 V is for example reported for [Fe(tacn)₂]^{3+/2+}; see: Wiegardt, K.; Schmidt, W.; Herrmann, W.; Küppers, H.-J. *Inorg. Chem.* **1983**, *22*, 2953.

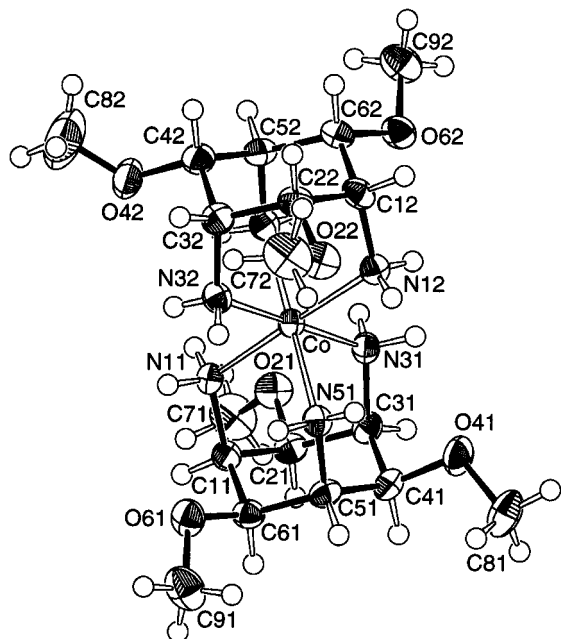


Figure 1. ORTEP drawing of $[\text{Co}(\text{tmca})_2]^{3+}$ (**5**) with numbering scheme and vibrational ellipsoids at the 50% probability level. The hydrogen atoms are shown as spheres of arbitrary size. $[\text{Fe}(\text{tmca})_2]^{3+}$ (**3**) is isostructural.

Table 5. Comparison of Selected Mean Bond Distances (Å) and Mean Bond Angles (deg) of the Fe^{III} and Co^{III} Complexes **1–6** with Esd's in Parentheses

| | 1 ^a | 2 ^b | 3 | 4 | 5 | 6 ^c |
|--------------------|----------------|----------------|----------|----------|----------|----------------|
| M–O | 1.964(9) | 2.011(3) | | 1.967(3) | | |
| M–N | 2.167(9) | | 2.014(7) | 2.152(4) | 1.984(6) | 2.000(8) |
| O–M–O ^d | 92.10(9) | 87.4(1) | | 91.5(1) | | |
| N–M–N ^d | 84.7(2) | | 89.3(9) | 84.5(2) | 89.7(8) | 89.7(10) |
| C–O–M | 117.1(9) | 121.3(2) | | 117.9(2) | | |
| C–N–M | 120.6(7) | | 119.0(3) | 121.3(3) | 119.2(4) | 119.4(2) |

^a Data from ref 2. ^b Data from ref 9. ^c Data from ref 11. ^d Intraligand.

lization experiments from wet EtOH always yielded visibly twinned crystals of the composition $[\text{Fe}(\text{tmca})_2]\text{Cl}_3 \cdot 5\text{H}_2\text{O} \cdot \text{EtOH}$. However, it proved possible to cut an untwinned platelet from one of the crystals and to use it for a successful structure analysis. The isomorphous crystals of $[\text{Co}(\text{tmca})_2]\text{Cl}_3 \cdot 5\text{H}_2\text{O} \cdot \text{EtOH}$ were also grown from wet EtOH. In contrast to the corresponding Fe compound, twinning was not observed. The crystal structures confirmed the presence of a hexaamine complex for both compounds (Figure 1). In both cases, one of the six peripheral methoxy groups and the methyl group of the EtOH molecule proved to be disordered.

It is of particular interest to compare mean Fe–O and Fe–N bond distances of **1** and **4** (mixed *fac*- FeN_3O_3 coordination) with **2** (FeO_6 coordination) and **3** (FeN_6 coordination) (Table 5). The short Fe–N distance of **3** (2.01 Å),^{24,25} which is slightly longer

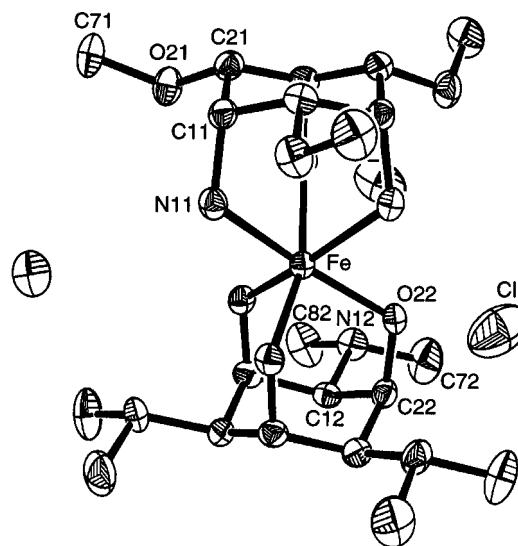


Figure 2. ORTEP drawing of $[\text{Fe}(\text{tmca})(\text{tdci})]^{3+}$ (**4**) with numbering scheme and vibrational ellipsoids at the 50% probability level. The hydrogen atoms are omitted for clarity.

than the corresponding mean Co–N length,²⁶ together with the spectroscopic and magnetic properties of **3** are indicative of a low-spin Fe^{III} complex.²⁵ On the other hand, the long Fe–N distance²⁴ in **1** has been attributed to a partial release of electron density from the deprotonated oxygen donors to the metal center by a $p_\pi \rightarrow d_\pi$ type bonding.² This trans influence of the strongly basic alkoxo groups would explain the enlarged Fe–O bond distance in **2** (FeO_6 coordination) relative to that in **1**.⁹ Exactly the same effect (i.e. a decrease of the Fe–O bond distance compared with **2** and an increase of the Fe–N bond distance compared with **3**) is also observed for the mixed complex **4** (Figure 2). The excellent agreement of Fe–O and Fe–N bond lengths in **1** and **4** thus further supports the idea that the short Fe–O and the long Fe–N bond distances in the mixed complexes are basically the consequence of an electronic effect. The Co–N distances in **5** and in the corresponding *taci* complex **6** are somewhat longer than the average Co–N distance of 1.965 Å reported for primary amines.²⁷ This elongation of the Co–N bond has been attributed to increased interligand repulsion between the hydrogen atoms attached to the coordinated amino groups.^{3,9}

An additional effect which deserves some discussion is the change in lipophilicity of the complex cations by adding methyl groups to the peripheral oxygen or nitrogen atoms. As shown previously, the bis-*taci* complex of Fe^{III} has a rather hydrophilic molecular surface with three hydroxy groups and three positively charged ammonium groups on the outside.² The introduction of 12 methyl groups in the *tdci* complex **2** generates a much more lipophilic periphery.⁹ In fact, this complex has a bipolar sandwich type structure with a hydrophilic pocket formed by the six coordinated alkoxo groups and the six N–H protons and a lipophilic shell formed by the two cyclohexane rings and the twelve methyl groups. In $[\text{Fe}(\text{tdci})_2]\text{Cl}_3 \cdot 15\text{H}_2\text{O}$, the hydrophilic pocket is completely filled with six water molecules, forming a second coordination sphere, and six additional water molecules, forming a third coordination sphere. A related bipolar, sandwich type structure is also found for the two *tmca* complexes **3** and **5** (Figure 3) and for the mixed complex **4**.

(24) For a variety of bis-*taci* complexes with MN_6 coordination, analysis of the structural data showed a linear dependence of the M–N bond distance on the ionic radius (see ref 9). According to this relationship, an Fe–N bond distance of 2.085 Å has been calculated for a hypothetical high spin $[\text{Fe}(\text{taci})_2]^{3+}$ complex with FeN_6 coordination.

(25) Only a few crystal structures of low-spin Fe^{III} hexaamine complexes have been reported. The Fe–N bond distances fall in the range 1.97–2.02 Å. See: (a) Marsh, R. E. *Acta Crystallogr.* **1987**, *B43*, 174. (b) Geilenkirchen, A.; Wieghardt, K.; Nuber, B.; Weiss, J. Z. *Naturforsch.* **1989**, *44b*, 1333. (c) Comba, P.; Sargeson, A. M.; Engelhardt, L. M.; Harrowfield, J. M.; White, A. H.; Horn, E.; Snow, M. R. *Inorg. Chem.* **1985**, *24*, 2325. (d) Bernhardt, P. V.; Comba, P.; Hambley, T. W.; Lawrance, G. A. *Inorg. Chem.* **1991**, *30*, 942.

(26) The observed difference in the M–N bond distances is in excellent agreement with the difference of the ionic radii of the octahedrally coordinated low-spin Fe^{III} and Co^{III} reported by: Shannon, R. D. *Acta Crystallogr.* **1976**, *A32*, 751.

(27) Orpen, A. G.; Brammer, L.; Allen, F. H.; Kennard, O.; Watson, D. G.; Taylor, R. *J. Chem. Soc., Dalton Trans.* **1989**, S1.

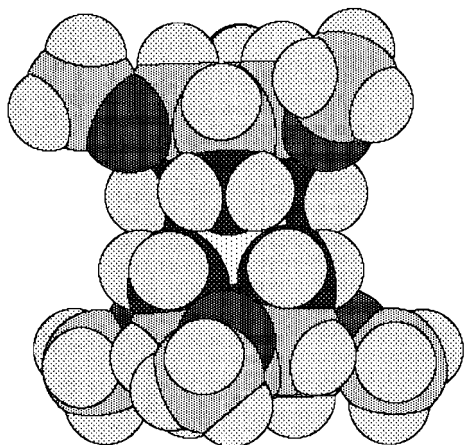


Figure 3. Space filling model (crystal structure) of $[M(tmca)_2]^{3+}$ ($M = Co, Fe$) showing the bipolar, sandwich-type structure having a lipophilic shell, consisting of the two cyclohexane rings and the six methyl groups, and a hydrophilic pocket, formed by the six coordinated primary amino groups. In the solid state, the hydrophilic pocket is completely filled with solvent molecules and Cl^- counterions (see Figure 4).

Again, the addition of methyl groups to the peripheral oxygen atoms generates a lipophilic shell and the coordinated donor groups form a hydrophilic pocket. The hydrophilic pockets are also completely filled with solvent molecules and Cl^- counterions (Figure 4). For the chloride salts of the Fe and Co complexes **3** and **5**, the second coordination sphere consists of one EtOH molecule, four water molecules, and one Cl^- counterion, which are all hydrogen bonded to the coordinated amino groups (Figure 4a). In $[Fe(tmca)(tdci)]Cl_3 \cdot 15H_2O$ (chloride salt of **4**), the hydrophilic pocket is filled by three Cl^- ions and three water molecules (Figure 4b). The additional water molecules of crystallization are connected by hydrogen bonds, forming an infinite net with characteristic $(H_2O)_{12}$ cages as building blocks (Figure 5). This arrangement of the water molecules in the $(H_2O)_{12}$ cage is closely related to the structure of ice.²⁸ The entire net has sufficiently large cavities to accommodate the complex cations which are connected to the $(H_2O)_{12}$ cages via their second coordination sphere by hydrogen bonding.

There is, however, a general difference between the arrangement of the solvent molecules in the bis-tdci and bis-tmca complexes. The hydrophilic pocket of the tdc complex **2** is basically generated by alkoxy groups (i.e. by proton acceptors) whereas the hydrophilic pocket of the tmca complexes **3–5** is generated by N–H protons (i.e. by proton donors) and so a different type of hydrogen bonding is found. This can be seen by the ability of the tmca complexes to bind anions like Cl^- , which would, of course, not be possible in a corresponding tdc complex such as **2**.

Another interesting feature of the complexes **1–6** is the different degree of distortion observed in their coordination spheres. The donor sets of the two tripodal ligands each define an equilateral triangle. The twist angle ϕ between these two triangles is a convenient parameter to describe the type of coordination polyhedron: $\phi = 60^\circ$ corresponds to octahedral geometry whereas $\phi = 0^\circ$ corresponds to prismatic geometry.^{25c,29a} It is well-known that low-spin d^6-Co^{III} has a strong preference for octahedral coordination due to the high ligand field stabilization. To a lesser extent, this is also true for low-spin

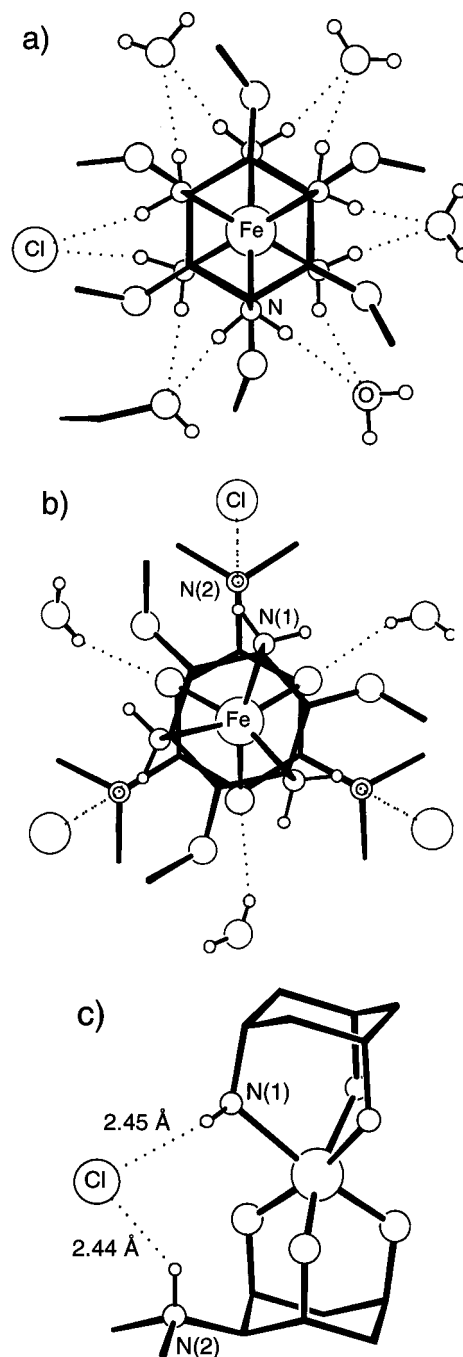


Figure 4. Illustration of the different coordination geometries of $[Fe(tmca)_2]^{3+}$ (**3**) and $[Fe(tmca)(tdci)]^{3+}$ (**4**). The carbon skeleton is represented by black sticks; H, N, O, Cl, and Fe atoms are shown as spheres with increasing diameter in this order. H–C atoms are omitted for clarity. A view along the (pseudo) 3-fold axis for **3** and **4** is represented in (a) and (b), respectively. In **3**, the six nitrogen donors have a trigonal antiprismatic geometry and the two cyclohexane rings have an eclipsed orientation. In **4**, rotation of one ligand around the 3-fold axis is required to get a minimal distance for the hydrogen bonds $N(1)-H \cdots Cl^-$. In (c) an additional view of the $N(1)-H \cdots Cl^- \cdots H-N(2)$ bonding scheme of **4** is given (only a part of the molecule is shown for clarity).

Fe^{III} . It is thus not surprising that no significant deviation from $\phi = 60^\circ$ is observed for the complexes **3**, **5**, and **6**. The complexes **1**, **2**, and **4** are high-spin d^5 , and therefore, no electronic preference for an octahedral environment over any other geometry is to be expected in terms of simple ligand field stabilization arguments.²⁹ Nevertheless, due to steric repulsions between the two donor sets of the ligands, an octahedral (i.e. trigonal antiprismatic) coordination mode should still be of

(28) Peterson, S. W.; Levy, H. A. *Acta Crystallogr.* **1957**, *10*, 70.

(29) (a) Arulsamy, N.; Glerup, J.; Hodgson, D. J. *Inorg. Chem.* **1994**, *33*, 3043. (b) Wiegardt, K.; Schöffmann, E.; Nuber, B.; Weiss, J. *Inorg. Chem.* **1986**, *25*, 4877.

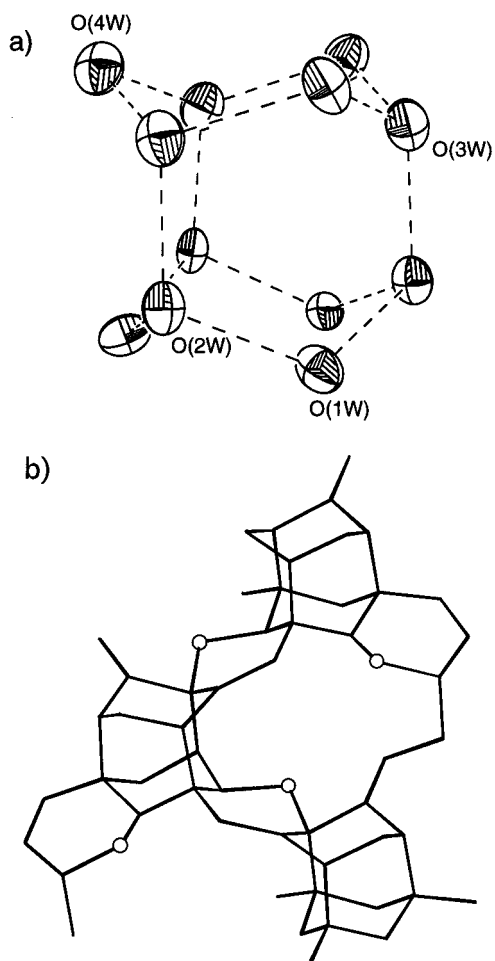


Figure 5. Structure of the waters of crystallization in $[\text{Fe}(\text{tmca})(\text{tdci})]\text{Cl}_3 \cdot 15\text{H}_2\text{O}$ (chloride salt of **4**). (a) ORTEP drawing of the $(\text{H}_2\text{O})_{12}$ cage with numbering scheme and vibrational ellipsoids at the 50% probability level. The hydrogen atoms are omitted for clarity. (b) View of a section of the indefinite net showing the large cavity for the complex cation. The linkage of the oxygen positions is represented by a stick model. The Cl atoms are shown as open spheres.

lowest energy. Indeed, in both complexes **1** and **2**, the twist angle ϕ was 60° within the level of significance. However, for complex **4**, a value of $41.6(1)^\circ$ was found, indicating a significant distortion toward trigonal prismatic coordination. A possible explanation for this unexpected result can be found by a close inspection of the above mentioned anion-cation interactions (second coordination sphere). The Cl^- counterions are hydrogen bonded by $\text{Cl} \cdots \text{H}-\text{N}$ interactions not only to the coordinated NH_2 groups of the tmca ligand but also to the peripheral $\text{NH}(\text{CH}_3)_2^+$ groups of the tdc ligand (Figure 4). The observed twist angle $\phi = 41.6^\circ$ corresponds to an optimal arrangement of the two ligands for this type of hydrogen bonding, indicating that the second coordination sphere of the high-spin Fe^{III} complex has a significant influence on its geometric properties.

Conclusions

The special versatility of taci is based on two chair conformations with either three oxygen or three nitrogen atoms in axial

positions. Selective methylation of taci results in the generation of ligands where only one conformer is available for tridentate binding to the same metal. Thus tdc is essentially a tridentate oxygen ligand, whereas tmca coordinates exclusively via three nitrogen atoms. The two types of methylated ligands can therefore be used to direct coordination modes which would not be preferred with taci. Since the steric properties of the *syn*-triaxial binding sites are similar for the three ligands, it is possible to elucidate the intrinsic electronic influence of oxygen and nitrogen donors on the properties of the central metal cation. The taci and tdc complexes **1** and **2** as well as the mixed complex **4** are high-spin and labile, whereas the tmca complex **3** is low-spin and inert. Clearly, it is only the N-ligand which generates the low-spin coordination and more than three N-donors are required.

Reports on hexamine complexes of Fe^{III} are rather scarce.²⁵ The low-spin $[\text{Fe}(\text{en})_3]^{3+}$ (en = 1,2-ethanediamine) has been described, but this complex is very unstable and hydrolyzes rapidly in aqueous solution.³⁰ For polyaza macrocycles, the stability of the Fe^{III} complexes is often significantly enhanced, and the crystal structures of the corresponding low-spin complexes with 1,4,7-triazacyclononane and 6,13-dimethyl-1,4,8,11-tetraazacyclotetradecane-6,13-diamine have been reported.²⁵ To our knowledge an X-ray structure of a hexamine complex of Fe^{III} with six primary amines has not yet been described. The high stability of **3** in aqueous solution is remarkable. In slightly acidic aqueous solution, no hydrolytic decomposition was detected, even after several days. However, the rapid decomposition at high pH indicates that the high resistance towards hydrolysis in neutral solution has a kinetic rather than a thermodynamic origin. This is in contrast to $[\text{Fe}(\text{en})_3]^{3+}$ which appears to be rather labile.²⁰ Analogous reactivity differences have been observed between $[\text{Ni}(\text{en})_3]^{2+}$ and $[\text{Ni}(\text{tach})_2]^{2+}$ (tach = all-*cis*-1,3,5-triaminocyclohexane).^{31,32} These can be attributed to the requirement for the cyclohexane ring to convert to the unfavorable boat conformation after dissociation of the first amine donor. A rapid recoordination rate would be expected because of this instability and because the amine group is never far from the metal ion. It is thus likely to be a combination of both a slower Fe-N bond rupture in the low-spin Fe^{III} condition and the conformational preference of the ligand which accounts for the kinetic inertness of $[\text{Fe}(\text{tmca})_2]^{3+}$.

Acknowledgment. We thank Dr. Andreas Hauser (Universität Bern) for helpful discussions and the reviewers for constructive advice. Financial support from Vifor (International) Inc. (St. Gallen, Switzerland) and from the ETH Zürich (Kredite für Unterricht und Forschung) is gratefully acknowledged.

Supporting Information Available: Listings of crystallographic data, anisotropic displacement parameters, positional parameters of hydrogen atoms, and bond distances and bond angles (13 pages). Ordering information is given on any current masthead page.

IC970291L

- (30) Comba, P. *Inorg. Chem.* **1994**, *33*, 4577.
 (31) Schwarzenbach, G.; Bürgi, H.-B.; Jensen, W. P.; Lawrance, G. A.; Monsted, L.; Sargeson, A. M. *Inorg. Chem.* **1983**, *22*, 4029.
 (32) (a) Read, R. A.; Margerum, D. W. *Inorg. Chem.* **1981**, *20*, 3143. (b) Shamsuddin Ahmed, A. K.; Wilkins, R. G. *J. Chem. Soc.* **1960**, 2901.